

Article

RFID Sensors for Monitoring Glazing Units Integrating Photovoltaic Modules

Mariusz Węglarski ^{1,*}, Piotr Jankowski-Mihułowicz ^{1,*}, Kazimierz Kamuda ¹, Patryk Pyt ¹, Grzegorz Pitera ², Wojciech Lichoń ³, Mateusz Chamera ³ and Cezary Ciejka ⁴

¹ Department of Electronic and Telecommunications Systems, Rzeszów University of Technology, ul. Wincentego Pola 2, 35-959 Rzeszów, Poland; kazik@prz.edu.pl (K.K.); p.pyt@prz.edu.pl (P.P.)

² Research & Development Center Bury, ul. Wojska Polskiego 4, 39-300 Mielec, Poland; grzegorz.pitera@bury.com

³ Talkin' Things, Al. Wilanowska 317, 02-665 Warsaw, Poland; wojciech.lichon@talkinthings.com (W.L.); mateusz.chamera@talkinthings.com (M.C.)

⁴ ALURON Sp. z o.o., ul. Okólna 10, 42-400 Zawiercie, Poland; cciejka@aluron.pl

* Correspondence: wmar@prz.edu.pl (M.W.); pjanko@prz.edu.pl (P.J.-M.); Tel.: +48-1785-44708 (M.W. & P.J.-M.)

Abstract: The paper focuses on the synthesis of semi-passive RFID transponders-sensors that are intended to integrate with active glazing units with built-in photovoltaic cells. The main purpose of the designed construction of the UHF RFID device is to provide diagnostic information in the monitoring system of a photovoltaic micro-power plant. Furthermore, the RFID sensor is aimed at being implemented at various stages of the product life cycle: production, distribution, storage, installation, common operation, service/maintenance and disposal. In the presented research work, particular attention is paid to several aspects of the RFID sensor synthesis: use of the energy, generated periodically in the PV cells, to power the monitoring device that has to act permanently; specification of the PV module parameters that have to be monitored in the diagnostic process; implementation of data acquisition and energy management models in an electrical circuit; wireless data transfer to the master unit (monitoring host), even in the absence of power supply (e.g., module damage, blackout), using a standardized communication protocol IEC 18000-63 used in the RFID technology; and the design of the antenna system taking into consideration limitations of electronic technology and the material properties of substrates and glasses used in PV modules and RFID sensors. Based on the results of the investigations, the modular structure of the RFID sensor demonstrator is proposed. Moreover, several diagnostic scenarios are analyzed in detail. On the basis of the provided considerations, it is shown that in order to find a malfunctioning component, it is enough to compare the voltages on the photovoltaic modules that are in the close vicinity.

Keywords: RFID technology; UHF RFID transponder; RFID sensor; active glazing unit; PV micro-power plant; PV glazing set



Citation: Węglarski, M.; Jankowski-Mihułowicz, P.; Kamuda, K.; Pyt, P.; Pitera, G.; Lichoń, W.; Chamera, M.; Ciejka, C. RFID Sensors for Monitoring Glazing Units Integrating Photovoltaic Modules. *Energies* **2022**, *15*, 1401. <https://doi.org/10.3390/en15041401>

Academic Editors: Lubomir Bena, Damian Mazur and Bogdan Kwiatkowski

Received: 23 January 2022

Accepted: 13 February 2022

Published: 15 February 2022

Publisher's Note: MDPI stays neutral with regard to jurisdictional claims in published maps and institutional affiliations.



Copyright: © 2022 by the authors. Licensee MDPI, Basel, Switzerland. This article is an open access article distributed under the terms and conditions of the Creative Commons Attribution (CC BY) license (<https://creativecommons.org/licenses/by/4.0/>).

1. Introduction

1.1. Explanation of the Main Aim

Photovoltaic (PV) modules are increasingly often integrated with glazing units that are installed in the facade walls of buildings. A typical glazing unit consists of several (two or more) panes, separated by gas chambers (i.e., filled with air or noble gases) [1]. If PV cells are integrated in the glazing unit, then an active glazing unit is obtained. It can be additionally equipped with a sensor module for monitoring its operation parameters. This solution can be used in a supervision system implemented in a micro-power plant. The authors suggest that the maintenance system should be based on RFID technology.

The synthesis process of an object-integrated, semi-passive RFID (radio frequency identification) transponder-sensor (RFID sensor) is a complex task. It is even more difficult when the RFID sensor is dedicated to be used in the active glazing unit and it is intended for

an automatic identification system covering all stages of the product life cycle: production, distribution, storage, installation, common operation, service/maintenance, disposal, etc. In the design process, particular attention should be paid to several aspects:

- selection of the operation parameters of the PV modules that are important for the proper diagnostics of the electronically marked object;
- implementation of the data acquisition and energy management model in an electronic control system;
- wireless data transmission to the master unit (host), despite the absence of power supply (e.g., PV module fault, blackout), using a standardized communication protocol of the RFID technology;
- design of the RF front-end of the RFID sensor, taking into account the technological requirements and dielectric parameters of the materials used (this problem was considered in [2,3]).

When considering the power supply conditions of the device, it should be noted that the illuminated PV module with a power of several hundred watts is an inexhaustible source of energy for the measurement systems based on the RFID technology. Furthermore, the use of active short range devices (SRDs) for data transmission is not a problem under such power conditions. Nevertheless, a monitoring system equipped with only such active transmitters stops working in the case of complete shading or damaging of the cells. In contrast, by using the RFID link, the acquired data can be available to service technicians even after the facade element is disassembled, and when the photovoltaic installation is completely damaged.

In order to achieve the assumed tasks, a modular structure of the designed RFID sensor demonstrator was proposed. It consists of:

- a module of object radio identification (RFID Part);
- measurement module (MEAS Part) that includes a data acquisition block with a wire interface (MCU Block) and a block of physical quantity sensors (SENS Block).

1.2. Monitoring PV Installation

The most important parameter of a single PV cell, and the entire module, is the current–voltage characteristic I - V (Figure 1a) [4]. The value of the current drawn from the PV source depends primarily on the intensity of the radiation that falls on the photovoltaic active surface. The output voltage at the open circuit and for the maximum electrical load varies only slightly with changes in the lighting. The maximum output power (at a given irradiance) is available at the bending point of the characteristics (Figure 1b). The maximum power point (MPP) is maintained by electronic circuits of the inverter that control the power fed into the electrical grid or used to charge batteries [5].

A typical PV module is the basic element of photovoltaic power plants and consists of several or a dozen or so cells [4]. The operating parameters of the device are determined by the internal structure and the arrangement of the PV cells [7]. As a rule, its output voltage is equal to several dozen volts. Therefore, it is necessary to combine several consecutive PV modules in order to increase the voltage value to the level that allows the connection to the power grid. Of course, the appropriate DC/AC inverter has to be used to adjust the power parameters. Further, successive strings have to be connected in parallel in order to raise the current efficiency of the micro-power plant. In this manner, it is possible to scale the micro-installation to the plant of any size. The key to the connection efficiency is to use the strings of the same parameters. Inconsistencies in the arrangements and operation disturbances, even in a single PV module, cause changes in the output parameters of the designed PV energy plants (Figure 1c). These problems are described in detail in [6].

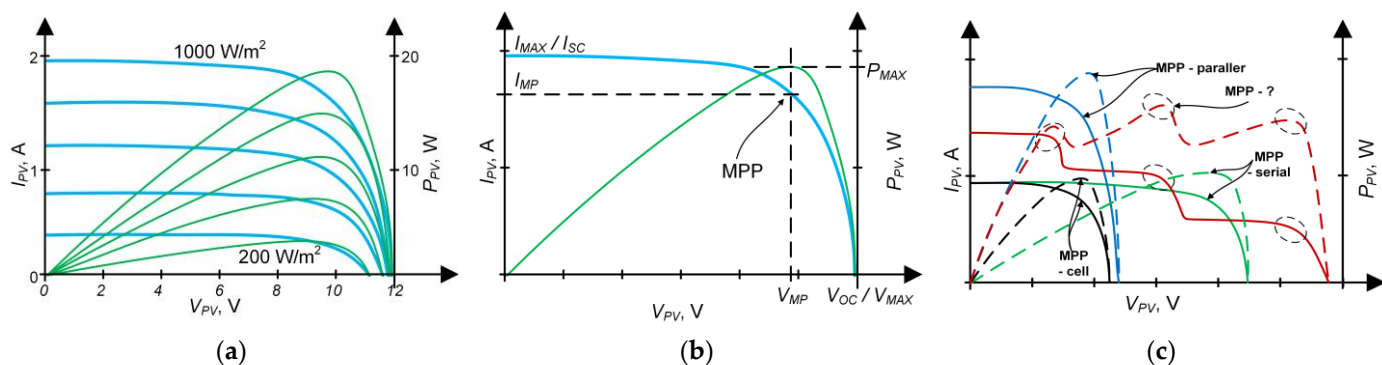


Figure 1. PV module operation parameters: (a) examples of I - V and P - V characteristics of PV module for lighting intensity from 200 W/m^2 to 1000 W/m^2 , in steps of 200 W/m^2 ; (b) basic operating parameters of the PV module, V_{MP} , I_{MP} —voltage and current of MPP at given solar luminance conditions, V_{OC} —voltage of open circuit, I_{SC} —current of short circuit; (c) changes in I - V and P - V characteristics in connection systems of PV cells: solid line—current, dot line—power, black—one cell, blue—parallel connection of two cells, green—serial connection of two cells, red—hypothetical curves of PV net configuration under environmental disturbances [6].

As can be easily noticed, it is essential that all the PV modules should operate at their maximum power point. This is not a problem when each of them has the same output I - V characteristics and operates under the same lighting conditions. Then, the MPP of the power plant coincides with the MPP of each single module, and the inverter can easily adjust the load conditions. Due to shading, local temperature changes, or negative environmental influences (e.g., aging, humidity, dirt, etc.), the PV modules may slightly differ in their parameters [8]. This can affect the efficiency of energy generation due to MPP shifting (Figure 1c, red line), and the voltage on the PV module output terminals may completely disappear or change polarity (which is prevented by protective diodes, but when it appears, the cells are cut off). As a result, the achievable energy is significantly reduced when at least one of the modules is not operating at its MPP. Therefore, the best, but very costly, solution would be to equip all modules with individual DC-DC converters with the possibility of tracking the operating parameters (MPPT function—maximum power point tracking) [9]. A much cheaper way to address these disturbances is to detect devices that do not work properly. This can be achieved using the monitoring system [10–12]. An extensive review of the methods applied at the inverter side and a new proposal to detect malfunctioning PV modules based on the electricity production analysis are given, for example, in [12]. Such methods are designed to detect almost all kinds of disturbances that affect the PV power plant. They can reveal that even one of the modules is malfunctioning. However, it is impossible to detect this faulty module by analyzing the parameters only on the inverter side. In order to identify a single element, the wire or wireless sensor network can be used as described in [10]. It is possible to use different communication systems (i.e., GSM, ZigBee, WiFi, RS485, USB, etc.) to send the diagnostic parameters, but they all have drawbacks. For example, in the wired network, it is necessary to build an extensive system of wired connections. The wireless monitoring system consists of many short-range devices that emit energy. In the case of micro-power plants on the facade walls of buildings, this can cause problems with electromagnetic compatibility. The generated electromagnetic field may disturb the activity of the electronics used inside the building. A detailed overview of the monitoring techniques used in PV systems is provided in [11].

1.3. RFID Technology in Monitoring Active Glazing Units

The authors suggest using the RFID technology to monitor the active glazing units. A standard implementation of the RFID system consists in attaching the passive RFID transponder to a marked object (e.g., PV module) in order to enable its identification based on a unique identification number [13]. Due to the use of a semi-passive transponder

equipped with an additional (usually battery) power source, first, the read/write range can be increased, and second, such a tag may be equipped with additional functional blocks. Attempts to replace the battery with other sources of energy (including PV mini-modules) can often be encountered in research works (e.g., [14]—research on new RFID chip, [15]—research on new RFID tag). In these cases, the PV module is an integral part of the RFID sensor. As the semi-passive transponder, such a sensor may be used to monitor the parameters of any object (including the PV plant components). Since producers of the RFID chips commonly embed temperature transducers into their products, the thermal images-based monitoring of PV modules is frequently examined in research implementations [16]. An attempt to use the RFID sensor to monitor the humidity level in the internal structure of the PV module is another example [17]. Detecting disturbances in thermal or humidity images certainly allows investigators to point out the damaged module.

In the publication, the authors show another method for detecting a malfunctioning module. The proposed RFID sensor is directly connected to the main terminals of the PV module, so that it is possible to supply the device with solar energy and to measure the value of the generated voltage. To summarize the review, it is possible to easily detect a damaged module using advanced solutions known in the RFID technology and by implementing proposed service algorithms.

Since it is important to obtain the largest possible interrogation zone (IZ) [18], the radiation coupling RFID systems should be used in the implementation under investigation. Such a system operates in the 860–960 MHz frequency range of the UHF band and its typical application consists of a software supervising part and hardware: a read/write device (RWD) and passive or semi-passive transponders. The essence of its operation is not only to exchange data with transponders but also to supply them with energy, via the electromagnetic radio waves generated by the RWD. When the voltage induced at the terminals of the tag antenna crosses the minimum level, the RFID chip is activated. Furthermore, according to basic principles of operation, its input impedance is constantly changing. The impedance is not equal to 50 Ω as it is in conventional radio systems. It is described by a complex number and depends on the parameters of the electromagnetic field, i.e., on the transponder location and orientation in a space, in addition to the presence of objects interfering with the magnetic field. It causes continuous changes in the impedance matching between the RF front-end and the antenna. The backscatter communication used to transfer data in direction from the transponder to the RWD [13] is also based on changes in this parameter. All communication mechanisms are implemented on the second-generation electronic product code protocol, the latest version of which is standardized by ISO/IEC 18000-63 [19]. It is also assumed that the effective power radiated by the RWD complies with the ETSI EN 302 208 [20] and does not exceed the value of 2 W ERP in the 865.6–867.6 MHz frequency band. In the American version of RFID systems, compliance with the FCC Part 15.247 standard is assumed [21]. Then the effective isotropic radiated power cannot be higher than 4 W EIRP in the 902–928 MHz frequency band. The above-mentioned features significantly complicate the design of the RFID sensor in the radio-communication aspects [22].

The proposed monitoring system is based on the semi-passive transponder. This construction consists of the chip and the antenna, in addition to the components that are used for impedance matching on the RF front-end. Additionally, the electronic circuit of the chip may be powered by a supplementary battery. Although this power source is not necessary for communication with the RWD, it can influence the size of the IZ. In new designs of the RFID chip, wire serial data interfaces (e.g., SPI, I2C) or sensors (most often temperature) are sometimes built-in [23]. These functions can be performed without the participation of the supervising system and provide, to some extent, autonomy of the tag. A comprehensive survey on the RFID technology and its contemporary applications is given in [24].

2. Materials and Methods

2.1. Analysis of the Application Environment

Before designing the RFID transponder-sensor, the impact of the identified object on the tag operation should be carefully studied. A spatial model and a cross-section of the most common active glazing units are shown in Figure 2: in the first cross-section the model with silicon cells (Si-PV) is considered, in the second that with dye-sensitized solar cells (DSSC) is shown. Since the reliability of the monitoring system is mainly dependent on the efficiency of the transponder antenna, the analysis should determine the dielectric parameters of the surrounding materials, such as glasses, polyvinyl butyral (PVB) layers, connecting wire nets, transparent conductive oxides (TCOs), and other functional layers. The electromagnetic field is also affected by the proximity of any metal elements of the structural frame. These components of the active glazing unit may disturb the communication in the RFID system and should be taken into account in the design process. The materials used to build the PV cells (both in Si-PV and DSSC modules) also exhibit a negative impact, but the cells usually do not cover the entire surface of the pane, so a separate place for fixing the RFID sensor can be found. The separation of 10 centimeters is enough to establish correct communication in the RFID system [3].

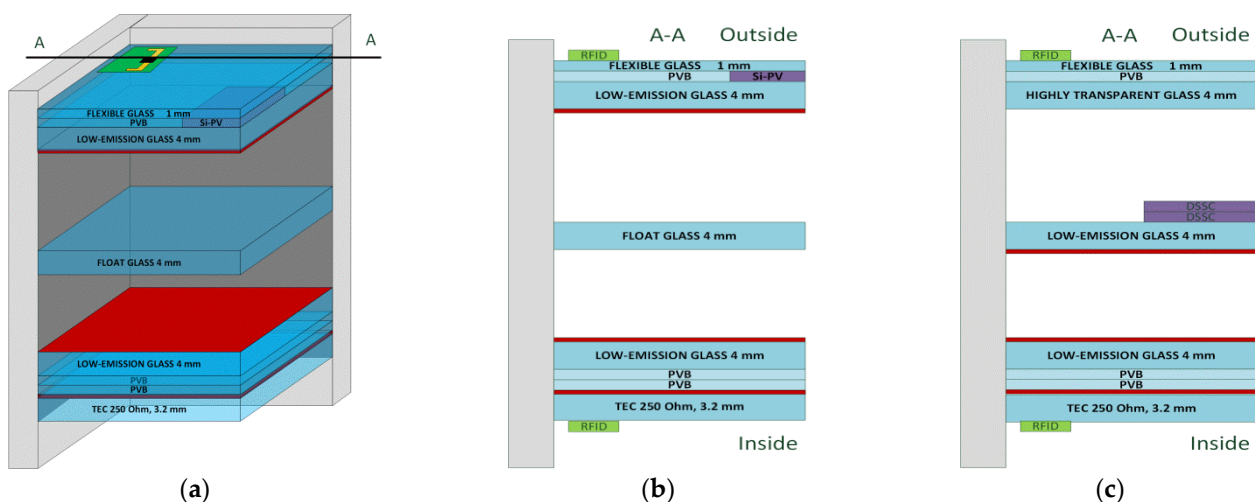


Figure 2. Models of exemplary active glazing units: (a) spatial model with Si-PV cells; (b) cross-section of model with Si-PV cells; (c) cross-section of model with DSSC cells. Real proportions are not respected for the sake of clarity of the drawings; TCO layers are marked in red.

Possible localizations of the RFID sensors (marked as RFID in the green box) are shown in Figures 2 and 3. Since the conductive layers shield the electromagnetic field, the two transponders have to be used in order to obtain identification in the RFID system on the both sides of the building facade. In such an arrangement, it is possible to design the RF front-end of the dedicated tag that works efficiently when applied to the specified active glazing unit [2]. In the case when the dielectric parameters of the functional layers are unknown (as, for example, in [25]), the harmful effect caused by these components can be, to some extent, neutralized by a plate of highly conductive metal (reflector). The reflector has to be taken into account in the antenna design model. The designed tag antenna can then be used to mark a wider range of products. Of course, the introduction of the reflector means that communication can only be established from one side of the unit. The location of the reflector depends on the capabilities of the technological process that is used to produce the glazing units. An effective solution is to embed the metal material into the PVB layer or to attach it to the inner laminated pane (Figure 3a).

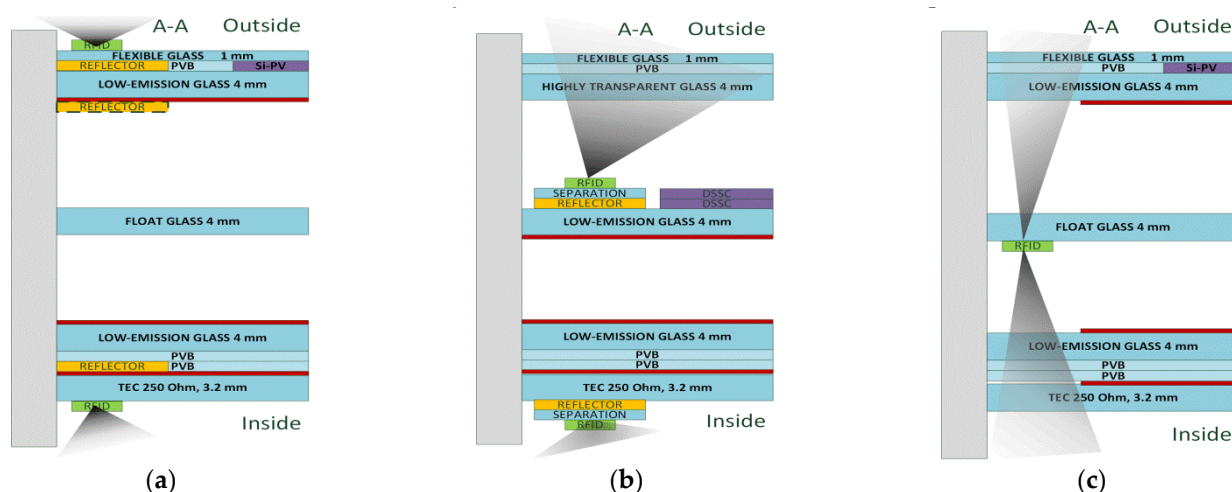


Figure 3. Localization of the RFID sensor in active glazing units: (a) implementation of RFID sensor with additional reflector; (b) structure of RFID sensor with additional reflector; (c) two-side communication after removing functional layer.

In the case of using the DSSC cells, it is also natural to consider the location of the RFID sensor on the inner pane (reading the identification only from the outside), as there is no reflective layer on the outer pane (Figure 3b). Some weakening of the radio wave propagation should be taken into account in the process of antenna design. On the other hand, the undoubted advantage is the native protection of the device against harmful environmental conditions. Furthermore, the RFID sensor can be developed as a completely independent construction that can be assembled at the stage of sealing the glazing unit. This leads to obtaining a universal device that may be applied on any package, regardless of the type of PV cells and functional layers used. The antenna structure with its own reflector is not sensitive to material modifications in the active glazing unit. It is also consistent with the hard tag constructions commonly used in the RFID technology. The integration of such a device can be carried out at the stage in which the active glazing unit is prepared for shipment from the production plant and consists in connecting the RFID sensor to the current terminals of PV cells.

Removing part of the functional layers in the vicinity of the antenna location allows the RFID sensor to be moved into the glazing unit and then it is possible to achieve two-side communication using only one device (Figure 3c). It also naturally protects the tag against the negative influence of environmental conditions. However, it should be noted that the effective and complete removal of functional layers in an industrial process is difficult and costly, and also causes a violation of heat transfer balances defined in industry standards.

2.2. Concepts of Electronic Circuit

The concept of the semi-passive RFID transponder-sensor assumes the use of the device at all stages of the active glazing unit life cycle. This requirement has a significant impact on the economic balance related to the costs of producing a complex electronic circuit of the tag. The benefits obtained will pay off in a very long period of time. Identification and technical data may be intentionally stored in the internal memory of the transponder for later use, and can be gathered autonomously by means of sensors monitoring the tagged object. At each stage of the life cycle (even after damaging the PV module), the information saved in the RFID sensor can be accessed wirelessly using a standard RWD.

Several designs of electronic circuits that could be used to create the RFID sensors were considered. For the investigation purposes, two main modules are distinguished. The RFID Part is designed as in a typical RFID transponder with special attention taken to maximizing the size of the interrogation zone. The main objective of the MEAS Part is to reach maximum functionality in the monitoring system at low cost and energy load

(Figure 4). The second part consists of two blocks (MCU and sensors) in order to facilitate implementation in the PV module. Ultimately, all components may be easily integrated into a commercial product.

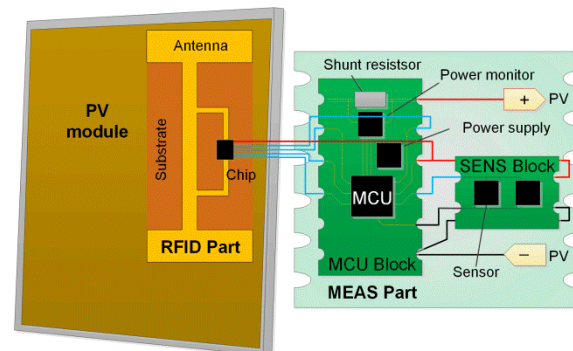


Figure 4. Block diagram of the RFID transponder-sensor.

The possibility of designing the RFID transponder (the RFID Part of the RFID sensor) dedicated to the glazing unit is considered in the publications [2,3]. The antenna system of the presented RFID sensor is developed to apply it with the AMS SL900A chip (AMS AG, Premstätten, Austria). The RFID Part is designed in the form of a sticker on a flexible substrate, which is intended to be placed in the space between the panes on the surface with the PV cells. It meets the requirements that are characteristic for the typical designs of RFID tags in terms of low production costs, easy integration with the object, and elimination of environmental influences.

The most important assumptions related to the MEAS Part concern its functionality, which is determined mainly by the proposed work scenarios for the supervision system of the PV micro-power plant. The construction of the electronic circuit, and thus the costs of its production, depend on the number of measured parameters, the accuracy of the sensors, the length of the operation cycle in the maintenance application, etc. The voltage and current should be measured under known environmental conditions, i.e., illuminance and temperature, in order to precisely indicate a faulty PV module. An electronic circuit with the ability to gather information on all of these characteristics is a sophisticated device compared to the capabilities of the typical RFID tag. It has to include a microcontroller (or another programmable logic device, e.g., FPGA) and an energy management system, in addition to digital sensors or analog transducers connected to an analog-to-digital converter (ADC, Figure 5). This means that the corresponding electronics are large and expensive to produce, and their disposal, together with the marked object, may be unprofitable. As a consequence, the MEAS Part has to be rather separated from the RFID Part, and both parts have to be linked by a wire interface. The modular structure has a negative impact on the reliability of the RFID sensor and complicates the installation and maintenance procedure. On the other hand, it can be easily hidden in the carrier frame of the glazing unit and also the access to the main PV module terminals is simplified.

Based on the analysis of the modern PV module characteristics and taking into account the requirements for monitoring systems of the active glazing units and micro-power plants on building facades, the authors suggest basing the maintenance of the system on measuring only the output voltage. A malfunctioning PV module can be easily found by referring the measured values to the standard I - V curve when the appropriate service routine by the authors is followed. Since all the PV chains should operate under the same environmental conditions, especially at the same temperature and illuminance, it is enough to compare the voltage on adjacent cells. The measured values have to be the same. Any deviation means that something is going wrong. If the service technician with a hand-held RWD would like to confirm the inspection results, he can additionally measure the temperature and illuminance. In this case, the voltage can be referred to the pattern characteristic that is provided for every PV module. This concept is the cheapest and

fully corresponds to the most important goal of indicating quickly and unambiguously a wrong cell. If the RFID sensor was minimized only to measure the voltage, then the target electronic system would be small, cheap, and easy to integrate with the RFID Part (Figure 5a). In this case, there is no need to move the MEAS Part into the frame of the glazing unit.

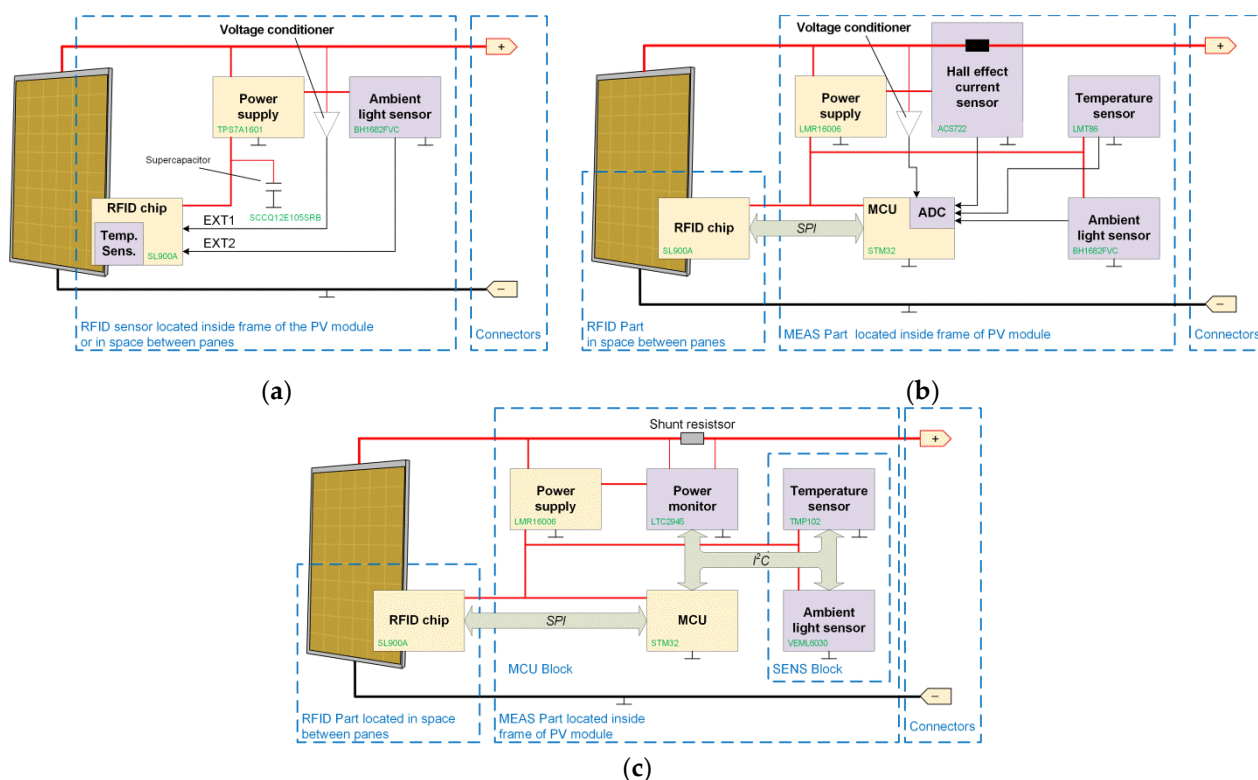


Figure 5. Block diagram of RFID transponder-sensor concepts: (a) device based on RFID chip; (b) device with microcontroller and analog sensors; (c) device with microcontroller and digital sensors.

However, intermediate constructions are also considered, especially in order to develop more advanced scenarios of the servicing system. The temperature measurement function can be implemented either by using the sensor built into the RFID chips or microcontroller, and by connecting the digital sensor through the serial wire interface or the analog transducer to an ADC. The SL900A supports all these solutions, and the accuracy of the standard electronics is enough for the designed application.

When measuring the luminous flux density (illuminance), the most important thing is to pay special attention to the spectral range of the transducer used. The measurements of this parameter are better based on a converter that is a reference section of the one of the photovoltaic cells. Such a transducer fits perfectly for integration into the PV structure of the active glazing unit. Nevertheless, it should be noted that measurement data correspond to the real value at the sensor location and may differ (e.g., due to surface contamination or shadow) for the PV modules even if they are in close proximity. This is the main reason why the maintenance procedure based only on the voltage measurements is proposed.

In all concepts of the RFID sensors, the assumption about the non-monitoring of current is made. The cost of implementing a converter adjusted to the output power of the PV module would be economically irrational. Moreover, to introduce the current transducer, modifications of wires in the main circuit are required. It should be noted that in a PV chain, the instantaneous current intensity is the same for all elements. It is thus even more pointless to duplicate the complicated and expensive measuring circuit.

A small number of chips can meet the application requirements: AMS (previously IDS) SL900A [23], Farsens ROCKY100 (Farsens, Donostia—San Sebastián, Spain) [26], EM Microelectronic-Marin SA EM4325 (EM Microelectronic-Marin, La Tène, Switzerland) [27],

or Cypress WM72016-6 (Cypress, San Jose, CA, USA, formerly Ramtron) [28]. The selected parameters of the chips, important from the point of view of the prepared implementation, are considered in detail in [22]. Since the energy harvesting from the electromagnetic field of the RFID system is enhanced by these ICs, the autonomous semi-passive RFID transponder-sensor can be developed. All products also provide the possibility of standard passive operation and battery-assisted mode—the PV module can be used as the auxiliary battery. Significant differences are primarily in terms of the user's memory size and the ability to link with peripheral devices (sensors). The WM72016-6 has the largest memory but it does not support the temperature transducers. The EM4325 and SL900A have similar functionalities. The advantage of the SL900A is the 10-bit ADC and a significantly larger memory size.

When the operation algorithm of these semi-passive chips is analyzed, it can be found that the power supply of electronic circuits in non-active PV modules causes a significant problem. The simplest construction (Figure 5a), without a microcontroller, cannot wake itself up after the power supply is turned on. Moreover, it is impossible to save the mode configuration in today's RFID chips when they are not supplied. The real-time counter (RTC) should also be powered permanently in order to maintain the time synchronization. Thus, the simplest designs have to be equipped with a supporting energy magazine, e.g., super capacitor. In the more sophisticated constructions (Figure 5b,c), a starting procedure can be applied to recognize daily cycles. Nevertheless, there is still a potential risk of error when the daily cycle is divided into parts (e.g., because of shading due to dark clouds). The only way to overcome this problem is to write all data with its own "Time Stamp". This requires the use of the RTC and additional memory resources.

2.3. Work Scenarios of Supervising System

The proposed operation algorithms of the RFID system implementation are called the work scenarios. The main purpose of the concepts elaborated for the RFID sensors was to minimize the number of elements in the electronic circuit, and to adjust the work scenarios to the size of the available memory and operating modes. Both the energy balance in designed electronic circuits and the utilization of hardware resources of the used components were taken into consideration. Further mentioned characteristics should also be taken into account in order to design the supervising system operating in a wide range of possible lighting levels.

The PV module is a source of electricity with an output voltage characteristic that varies in the time domain. The highest value is obtained only when the cells are fully illuminated, which most often occurs about noon (with relation to the solar time) or in the middle of the daily cycle (when the panels are oriented in a direction other than south). However, this characteristic strongly depends on many factors i.e., latitude, cloud cover, precipitation, air pollution, contamination of the active surface, obstacles reducing the surface of energy absorption, temperature, time of day and year, etc. The maximum output voltage can usually be obtained at different times of the day. However, it is possible to find a middle point on the daily characteristic.

The voltage at the PV module terminals is a native parameter that is available for monitoring tasks without the need to implement any additional connections (the ICs must be just powered). Nevertheless, knowledge about the other operating parameters (i.e., temperature, lighting intensity, current intensity, current measurement time, etc.) may help to estimate the lifetime and reliability of the module in the long term. The implementation of additional sensors, however, is associated with the complication of the electronic system. For example, it is necessary to solve a number of technological problems related to the correct selection of the localization for assembling transducers of measured quantities. Moreover, sensor protection against environmental conditions, in addition to a significant modification of the active glazing unit manufacturing process, has to be predicted.

Therefore, monitoring the condition of the cells by comparing only the voltage values with a known reference characteristic seems the most promising scenario of the PV module

diagnostics. The characteristics of different examples of active glazing units in a common chain indicate minor discrepancies in their operating parameters (Figure 6a). If they are compared with the reference characteristic determined in the laboratory stand, it is possible to detect a faulty or an excessively worn element. Unfortunately, this method has a fundamental disadvantage because measurements performed in a real application usually differ from those used to determine reference parameters on the laboratory site. Although calibration can be performed on the target application, this task is not economically acceptable in practice due to the large number of measurements that should be made for various external conditions (day time, seasons, temperature, exposure, etc.).

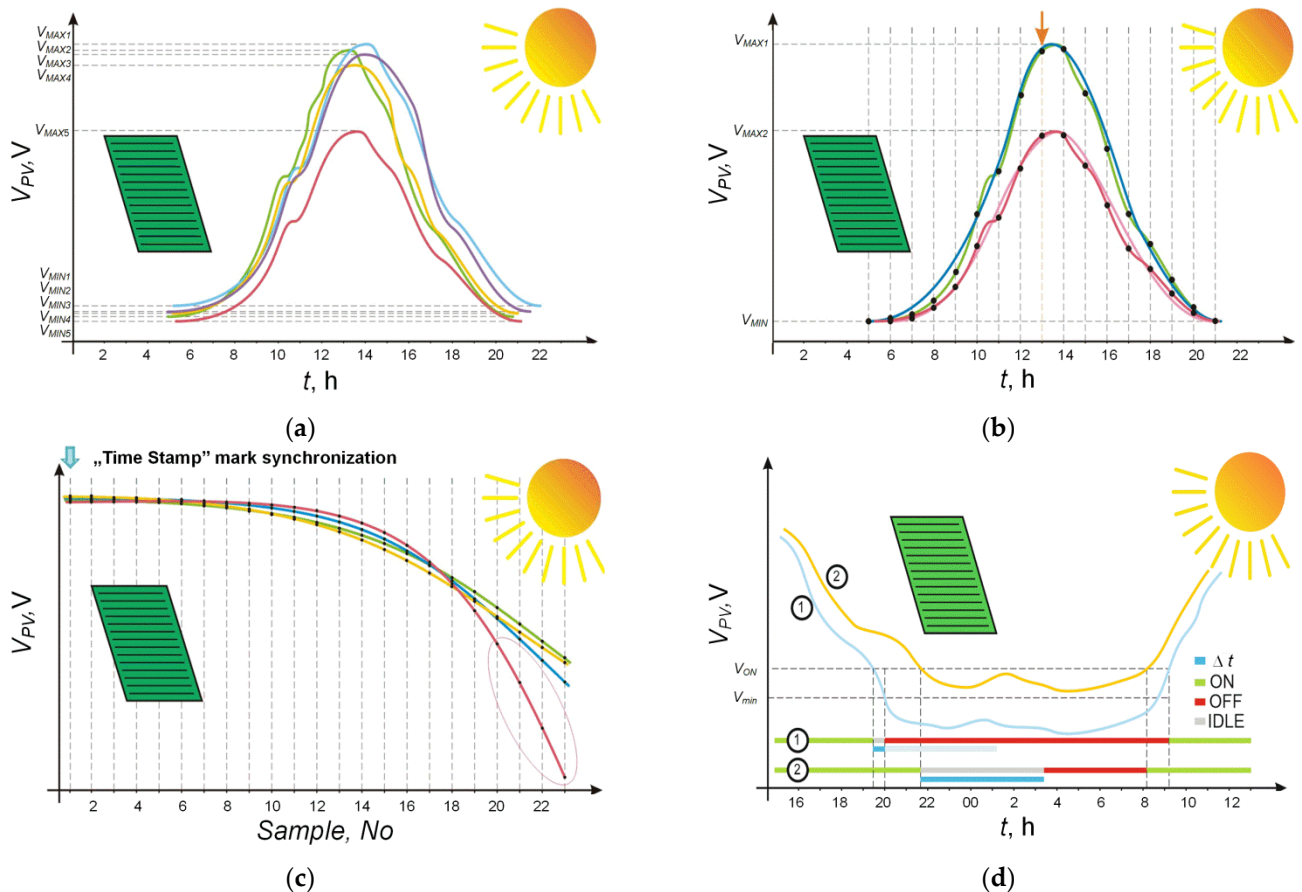


Figure 6. Exemplary $V_{PV} = f(t)$ characteristics: (a) voltage at PV module terminals in similar lighting and environmental conditions; red line—malfunctioning module; (b) approximation of voltage characteristic, quasi-maximum measurement in 24 h intervals is pointed by arrow; (c) interpretation of diagnostic results, quasi-maximum values are in descending order; (d) operation of RFID sensor depending on output voltage level disturbances; voltage lower than V_{min} (1) and voltage higher than V_{min} (2) of supply voltage; Δt —time for the safe shutdown of the RFID sensor; ON/OFF—switching the system on/off; IDLE—termination of measurements in the daily cycle; V_{ON} —threshold voltage of DC/AC inverter; V_{min} —minimal supply voltage of RFID sensor.

The service technicians are basically not interested in the absolute values of the individual parameters. However, they want to know if the PV module works correctly. The entire system works properly if the individual PV module generates the voltage and current compliant with the technical specification within the acceptable limits of the parameter discrepancies. Then, an automated inverter equipped with control and management functions supplies energy to the receiving system without reporting unjustified drops in the generated power. If the inverter was equipped with, e.g., alarm functions for exceeding parameter limits or in external sensors of temperature and light intensity, it may only raise an alarm for the failure of the connected chains as a whole. The problem arises when we

want to find the module in a given assembly that is subjected to accelerated deterioration or failure (Figure 1c). This can be detected only during the periodic maintenance, after disassembling the chain.

The authors propose to perform diagnostic based on the comparison of the voltages on PV modules in the close vicinity, but, of course, under the same environmental conditions. In this scenario, it is important to predict the proper moment of the RFID sensor awakening within daily cycles, to determine the unequivocal voltage value that represents the measured segment of the $V = f(t)$ characteristic and to minimize the amount of saved data. Since the MEAS Part can be safely woken up after crossing the threshold voltage V_{ON} , the impulse turbulences at the output of the PV module causes a significant problem, i.e., it disturbs the determination of the beginning and end of the daily cycle (Figure 6d).

The registration of the voltage characteristic consists in performing a series of measurements at fixed intervals (Figure 6b). The diurnal characteristics can be determined with various degrees of accuracy and the time intervals can vary from fractions of a second to a single measurement during the day. The greater the number of points, the more accurately the curve can be reproduced, but the amount of data to saving also increases. However, the total number of recorded bytes in the autonomous RFID sensor is severely limited by the memory capacity. Therefore, the introduction of sample filtration should be considered for practical reasons. This can be done by increasing the frequency of the measurements and only recording the average value over a fixed “sampling” time. A series of daily measurements can also be replaced with an approximation curve. Both methods are relatively easy to implement in the microprocessor computing block, and they also help to eliminate transient disturbances in the illumination. The acquired data may be processed in external databases in order to perform diagnostic tasks in a much wider range.

The method of data filtering cannot be used in the simplest design of the RFID sensor (Figure 5a) due to the lack of the microprocessor and the relatively small memory capacity available in the RFID chips. In this case, the authors propose the method consisting in performing the single measurement of output voltage at intervals of 24 h, triggered by the RTC. This allows the acquisition of the monitoring time even over a year, depending on the measurement resolution and available memory on the RFID chip. To enable this, the corresponding “Time Stamp” mark must be inserted into the data memory when the supervising system is commissioned (Figure 6c). In the simplest case, it can be, e.g., the daily date of the beginning of the monitoring period, supplemented by the sample numbers. Even if it is not possible to precisely set the measurement moment at the maximum daily voltage, the trend of changes in long-term durability will be visible for a long period of time. Thus, the device diagnosis can be based on the comparison of neighboring cells in the PV chain (Figure 6c). If the curves coincide, it can be assumed that the sources behave correctly. Accelerated degradation of the malfunctioning module (red curve) stands out from the rest of the observations.

The proposed method can also be used in the system with the advanced computing block (Figure 5b). The maximum value may be determined for the daily curve and recorded in the memory for long-term monitoring periods. The detailed data should be deleted or stored for a shorter time (e.g., 1 week), which would guarantee the service access to additional information in the event of an ad hoc inspection.

The idea of the monitoring system operation consists in a direct comparison of the output voltages on the cells in the PV chain that work under the same environmental conditions. The condition of the same illuminance and temperature would be met if the synchronization of the measurement moment on all MES Parts was ensured. As this is impossible, the averaging of the data over a period of time is provided. On this basis, the daily cycles are recognized and the time stamps are estimated. In addition, the amount of information stored in the RFID chip memory is reduced.

If the averaging calculations have to be performed, a system that is based only on an RFID chip (without a microcontroller) cannot be applied in practice. At the current level of the RFID technology advancement, the microcontroller is necessary at least for initializing

the data acquisition. However, since a microprocessor is implemented, it is better to use it for all computing and management tasks. It is also possible to exclude the analytical functions from the MEAS Part and implement them in the software that controls the RWD device or in a database application. Due to the restrictions of the memory resources, the RFID system can also work in the online mode, and the determination of the parameters and identification of degraded elements is executed on the basis of the current daily cycle analysis.

The concept in which the voltage measurement is carried out only during the maintenance service (both related to the periodic inspection and the fault diagnostics) is also considered. The measurements can be initialized and passed to the handheld RWD during the inspection. Then, the degree of PV module degradation can be detected on the basis of the measured voltage values. It can be performed by comparing the voltage on the PV modules in the same chain or by relating the measurements to the I - V characteristic for a given illuminance and temperature. Such a system can be based on the RFID chip, and no additional power source or advanced microprocessor-based computing block is necessary. This concept is the cheapest and fully corresponds to the most important goal of quickly and unambiguously indicating the damaged PV module.

3. Results

3.1. Versions of Developed RFID Sensors

Two versions of the RID sensors were designed on the basis of the presented discussion. In the first laboratory development demonstrator (Figure 7a), the MEAS (PA001) and RFID (PA003) Parts are clearly separated. Additionally, the board with measurement interface (PA002) for external sensors is designed. The multi-criteria investigations can be performed in such a construction, i.e., on device functionality in the active glazing unit applications, in the scope of acquisition model development, energy balance calculations, or finding improvements in operation scenarios. The PCBs can be modified independently, of course, taking into account the specific requirements for communication interfaces used in ICs (e.g., SPI in SL900A, STM32).

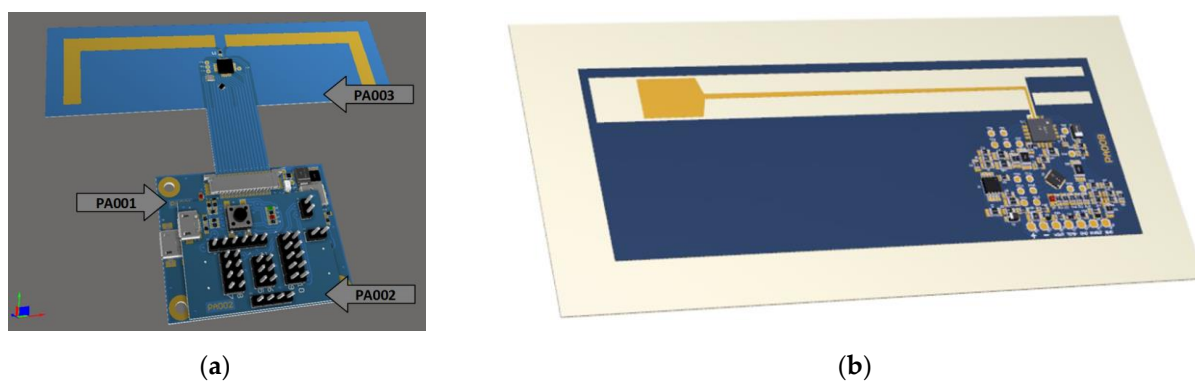


Figure 7. Two versions of RFID sensor: (a) research system based on three PCBs: PA001—MEAS Part, PA002—research interface part, PA003—RFID Part; (b) single-board device.

The ARM Cortex-M STM32 (ST Microelectronics, Geneva, Switzerland) is used in the design. This choice with such large hardware resources is only for research purposes and can be replaced by a much simpler IC. However, the STM32 provides ample memory for saving data gathered about the PV system and offers sufficient computing performance for the advanced data processing, in addition to access to multiple I/O ports, thus allowing designers to expand the measurement circuits. Despite its high complexity, it still consumes a little energy as unused microcontroller blocks can be easily turned off. This choice should be taken as an example, because most of the microcontrollers, both 8-bit and 32-bit versions, meet the requirements of the destined application. Nevertheless, the ICs should

be dedicated to low-power implementations; they should also be equipped with typical serial interfaces (e.g., SPI or/and I2C) and analog-to-digital converters.

Moreover, the remaining blocks of the MEAS Part (voltage converters, light intensity, and temperature sensors) should be selected to be adequate to the design needs, taking into account economic conditions and producers' capabilities. The temperature and the light intensity sensors can be physically integrated on the PA003 board. PA003 is intended to be manufactured on a flexible substrate and placed in the inter-pane space of the glazing unit. This localization has the smallest limitations in the propagation of radio waves, and the measured physical quantities can directly affect the transducers. Nevertheless, since the digital interface is used between sensors and SL900A, the PA001 and PA003 boards can be developed independently. The entire device is powered by the energy generated by the PV cells. Therefore, it has to be connected to the main wires of the PV module, which naturally permits measurement of the voltage signal.

The resolution of the measuring system depends primarily on the adopted work scenario, diagnostic assumptions, and the operation algorithm controlling the ADC. The measurement block is based on the 12-bit ADC of the STM32L432 microcontroller. The maximum voltage generated by the PV module does not exceed the value of 60 V. Since the rate voltage at the analog input has to be within the range from 0 to 3.3 V, an appropriate voltage divider is used. The results of the ADC processing obtained with the 12-bit resolution can be easily converted into the instantaneous values of V_{PV} expressed in mV. They can be returned in the diagnostic RFID system in the case of ad-hoc measurement scenario.

It is important to have access to the acquired data even in the event of damage to the PV panel, i.e., the auxiliary supply source. In such a situation the microcontroller does not work, but the RFID tag can always be read. Assuming the diagnostic scenario, e.g., data storage for one year and lack of module synchronization, in the search for the maximum value the measurements should be performed, e.g., at intervals of several ms (with a frequency greater than the load changes resulting from the inverter operation algorithm). On the basis of N measurements, a moving average should be determined, and then the maximum value should be designated and written in the RFID chip memory. To further save memory space, the data can be compressed to 8 bits, i.e., the resolution will drop to about 250 mV. Nevertheless, it is still a value that significantly exceeds the diagnostic needs. As in many ADCs, a large number of main errors also have an effect on the performance of the MEAS. Part. Nevertheless, even summing up (although not fully justified) these errors, the total uncertainty will not exceed the value of a few LSB. It should be emphasized that the proposed diagnostic method is a comparative method, so the absolute value is not important, provided that identical measurement conditions are maintained. In addition, it involves the analysis of many measurements collected over a long period of time. The service technician should only react to a significant deterioration in the PV module parameters (e.g., level of approx. 10%, a few volts), because it involves its costly replacement.

The single-board RFID sensor (Figure 7b) was also designed for integration into the real application of the active glazing building facade. The device is limited to the basic assumptions of the supervising system and meets the requirements for the common RFID tag. First, the possibility of voltage measuring is ensured. Additionally, the inputs for temperature and illuminance sensors are provided (Figure 8).

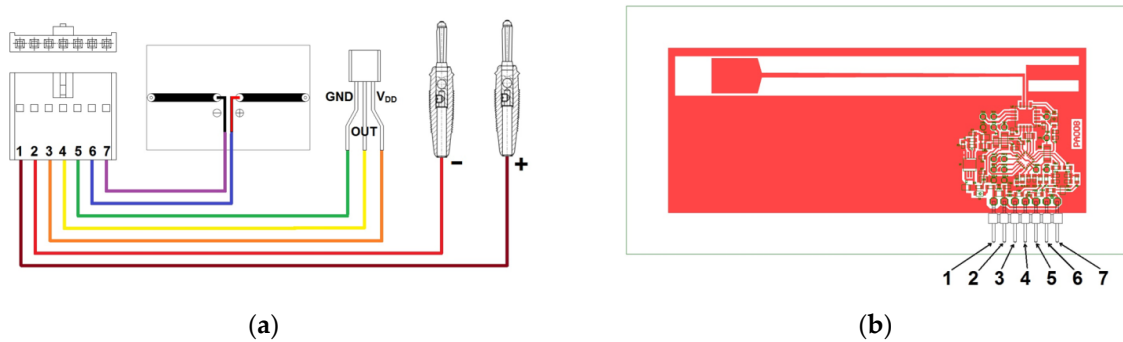


Figure 8. Single-board RFID sensor: (a) wire interface for implementation in active glazing unit; (b) input description: 1—PV cells “+”, 2—PV cells “−”, 3— V_{DD} for external temperature sensor, 4—input for ext. temp. sensor, 5—GND for ext. temp. sensor, 6—“+” for ext. illuminance sensor, 7—“−” for ext. illuminance sensor.

The integration of the RFID and MEAS Parts consists in fabricating the electronic circuits on a common substrate, where the bottom layer is clad with a Cu layer. The reflector is used to eliminate the influence of materials (from which the glazing unit is made) on the propagation of electromagnetic waves. The development of a new construction is associated with redesigning the antenna, digital electronic circuits, and power block (Scheme S1). It should be noted that all electrical wires are made on the top layer. This allows for full integration of the demonstrator with the glazing unit, i.e., making the elements directly on the glass by the screen printing used in the production stage [2].

The integration of the RFID sensor with the active glazing unit can be carried out when the product is prepared for shipment from a factory. It consists in connecting the voltage input in parallel with the main terminals of PV cells and inseparably fixing the flexible tag to the surface: external or internal, depending on which side of the facade the service should be provided. If there is a need to ensure communication from both sides, then two RFID sensors may be used.

A complete evaluation of the destined application was carried out with the simplified constructions. The possibilities of modifying system functions and work scenarios for the real application of the active glazing unit are also indicated. It should be emphasized, however, that the designed system is fully functional and can be directly used in the target products.

3.2. Evaluation and Result Discussion

The process of evaluating the final RFID sensor was carried out on 10 test boards of the model shown in Figure 7b. Nevertheless, the demonstrator in Figure 7a was used as the advanced demonstrator in the auxiliary investigations.

3.2.1. RF Tests

The most important part of RFID devices is the antenna system. It was designed according the rules elaborated in previous publications [3,29]. The 10 development sensor boards were tested under both laboratory and quasi-real conditions.

As it was explained in [3], the antenna impedance Z_{TA} and the power transfer coefficient CMF have to be determined in order to evaluate the RF parameters of the RFID transponder. These parameters are presented in Figure 9. Analyzing the data obtained on the basis of numerical calculations and measurements, it can be seen that the shape and nature of the resistance and reactance diagrams converge (Figure 9a,b). However, a slight shift in the frequency domain between the model and the measured results is noticeable.

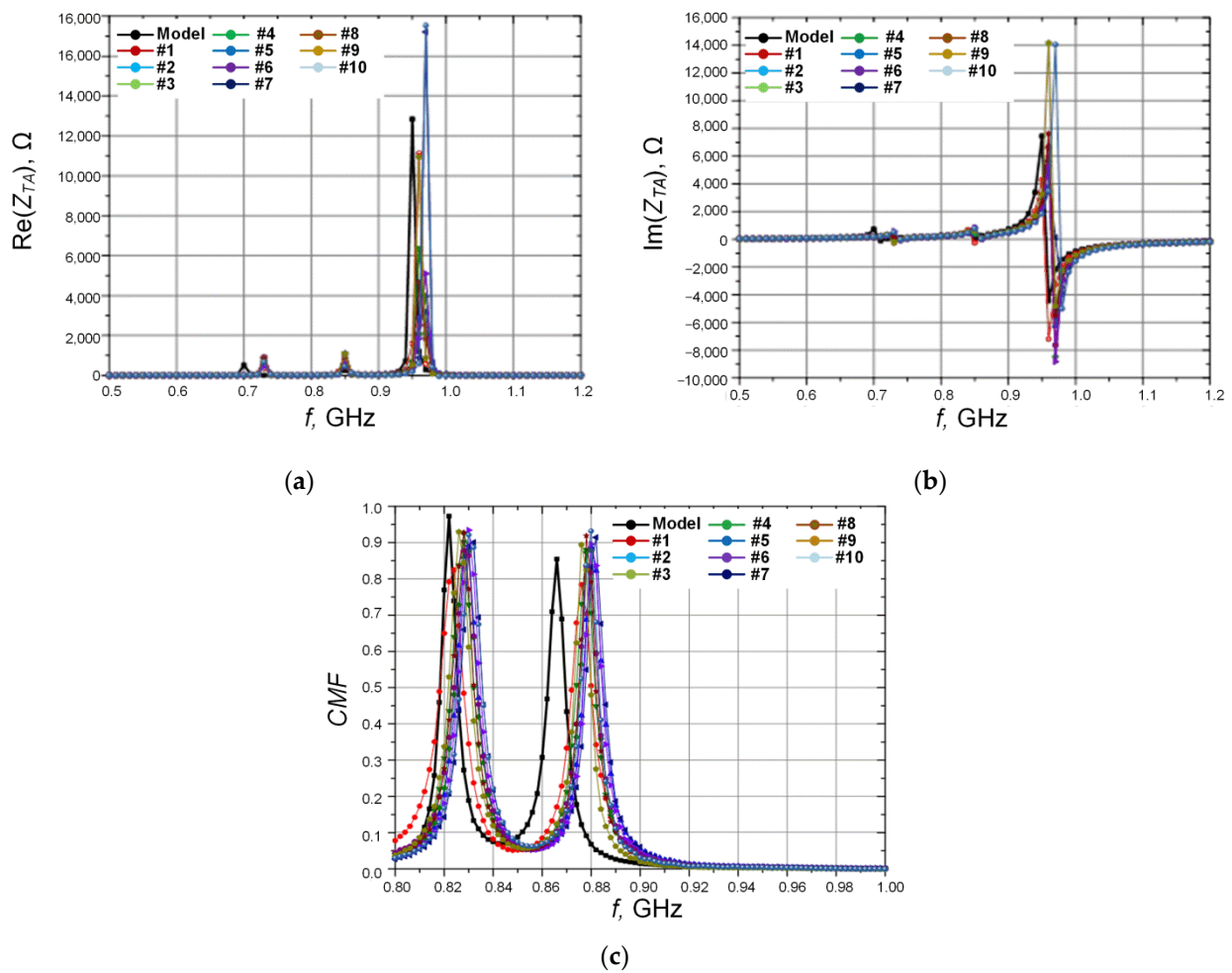


Figure 9. Parameters of RF front-end in RFID sensor under tests: (a) antenna impedance Z_{TA} —resistance; (b) antenna impedance Z_{TA} —reactance; (c) power transfer coefficient CMF .

Inaccuracies in the input dielectric parameters assumed in the calculations are the source of these inconsistencies. The relative permittivity ϵ_r and dielectric loss $\text{tg}\delta$ of the microwave laminate estimated on the basis of producer datasheets are given with an approximation in the frequency domain. Furthermore, there is a discrepancy between the values measured for the subsequent samples. This is due to the slight differences in antenna dimensions caused by uncertainties in the fabrication process. Neither discrepancy affects the correct operation of the RFID sensors in the target application [3]. The shift in the measurement results in relation to the calculations is also visible in the case of CMF (Figure 9c). Nevertheless, the curves have a similar shape, and the maximum values occur for similar frequencies in all of the samples. Again, this proves the convergence of the obtained results.

The convergence of the characteristics confirms that the design process was developed properly. First, the impedance of the antenna is coupled to the impedance of the chip. This means that real parts of the impedances are equal, and the imaginary parts are of the opposite nature (chip—capacitive and antenna—inductive). In turn, the CMF factor shows the degree of matching of both impedances. $CMF = 1$ means full matching, i.e., all energy obtained in the antenna circuit is transferred to the harvester in the chip. The graphs clearly show the shift of the measurement data for 10 samples in relation to the calculation model. Nevertheless, the shift is so small that the developed sensor can work properly in the target application. Certainly, the increased attenuation of the signal due to the impedance mismatch negatively affects the read/write range. This means that if the errors causing the mismatch were eliminated from the production process, the sensor

would be even more suitable for the proposed application, i.e., the read/write range would increase.

The directional diagrams of the radiation pattern are another parameter that is the subject of the special attention during the laboratory tests (Figure 10). Since the passive reflector is placed under the antenna radiator, the radiation pattern is directional. It is also not symmetrical (the main beam is significantly wider in the horizontal H plane than in the vertical V plane) due to the unusual design of the monopoly antenna. The described shape of the radiation pattern may have an impact on the transponder read range if the tag is positioned at an angle according to the RWD antenna.

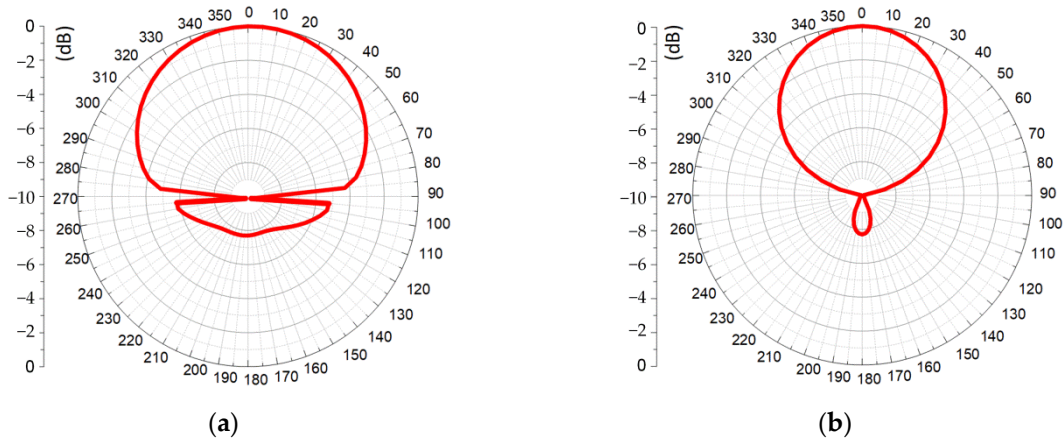


Figure 10. Directional diagrams of the RFID sensor: (a) horizontal plane H; (b) vertical plane V.

3.2.2. Read Range Tests

The read/write range (r_{PwrMax}) is the main factor of the RFD sensor effectiveness in the target application [13]. It was determined in an anechoic chamber under specified test conditions (Figure 11d): voltage V_{BAT} of the extra power source that supplies the RFID chip and circuit of the MEAS Part; the output power P_{RWD} of the RWD. First, the read range of the test samples is not constant for the selected RWD output power level (Figure 11a). In the semi-passive mode at $V_{BAT} = 15$ V, a significant increase in the r_{PwrMax} is confirmed. The read range is larger than in the passive mode ($V_{BAT} = 0$ V), even if the minimum output power is delivered. This is because the sensitivity of the SL900A increases when the chip works with an auxiliary power supply. It should also be remembered that the orientation of the transponder antenna in relation to the RWD antenna has a significant impact on the read range (Table 1).

Table 1. Read range r_{PwrMax} of test samples 5 and 6 for RFID sensor deflection, $V_{BAT} = 0$.

Sample, No	Angle	P_{RWD}, W	P_T, W	ERP, W	r_{PwrMax}, m
5	−45	0.5	0.47	0.63	0.39
	45	0.5	0.47	0.63	0.24
	0	0.5	0.47	0.63	0.45
	−45	1.4	1.18	1.57	0.61
	45	1.4	1.18	1.57	0.43
	0	1.4	1.18	1.57	0.70
2	−45	0.5	0.47	0.63	0.37
	45	0.5	0.47	0.63	0.24
	0	0.5	0.48	0.64	0.41
	−45	1.4	1.18	1.57	0.61
	45	1.4	1.18	1.58	0.41
	0	1.4	1.18	1.61	0.81

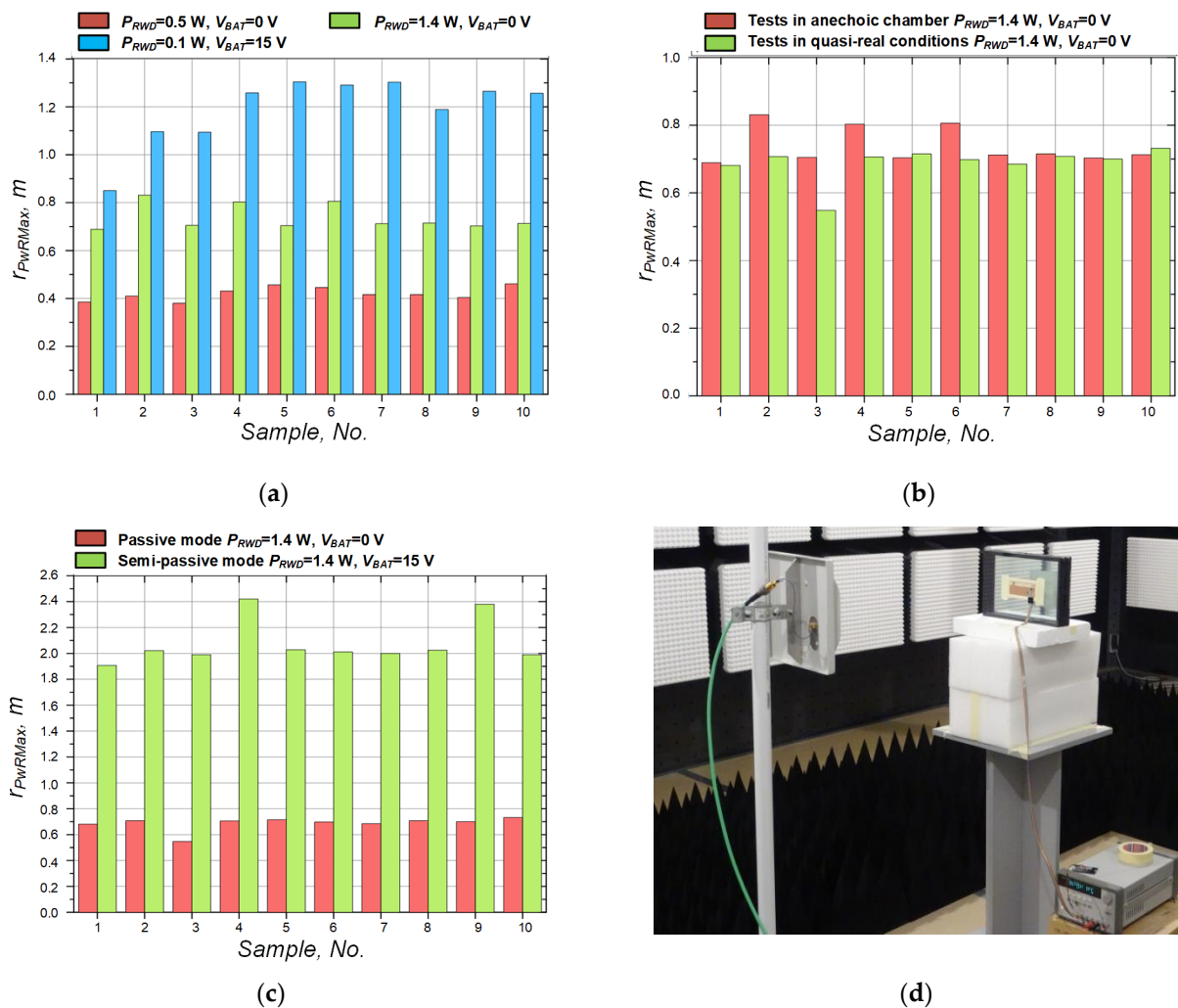


Figure 11. Read range r_{PwRMax} of test samples: (a) determined for different values of output power of RWD P_{RWD} and voltage on auxiliary power source V_{BAT} ; (b) comparison of tests in anechoic chamber and in quasi-real conditions; (c) tests of passive and semi-passive mode in quasi-real conditions; (d) laboratory stand in anechoic chamber; inaccuracy of measurement method $\pm 1\text{ cm}$.

The influence of the marked object (AGC Stopray Vision-50 triple glazing unit) on the performance parameters of the tested samples was also checked in the anechoic chamber (Figure 11b). The RFID sensors were placed in the center of the pane covered with the TCO layer. The measurements were performed for the maximum output power $P_{RWD} = 1.4\text{ W}$ of the RWD, which is consistent with the ETSI EN 302 208 standard. On the basis of the obtained results, it can be concluded that the proposed construction of the RFID antenna is resistant to the influence of the materials from which the active glazing unit is manufactured. Despite the close proximity of the unit surface, the measured read range is almost the same. The noticeable slight discrepancies can be explained by the imperfection of the measurement method. A similar comparison was carried out for the measurements at two operation modes of the RFID chip: passive and semi-passive (Figure 11c).

3.2.3. Outside Tests

The operational functionalities, especially of the MEAS Part, were also tested in the PV module application (Figure 12). A special grid-off micro-plant consisting of a PV module, a Skymax Expert MEX 1.5K-12 (Skymax, Wrocław, Poland) inverter, and an accumulator for energy storage was prepared. The operating parameters were monitored by the external acquisition system based on LASCAR EL-USB-3 data loggers (Lascar Electronics, Wiltshire, UK), for a period of 10 days. In order to measure the full characteristics of the PV module

(the maximum power of the module used in the tests is approximately 317 W), a precise electronic load ARRAY 3723A (Array Electronic, Nanjing, China) was used. Although the test process was time consuming, a number of important data were obtained.

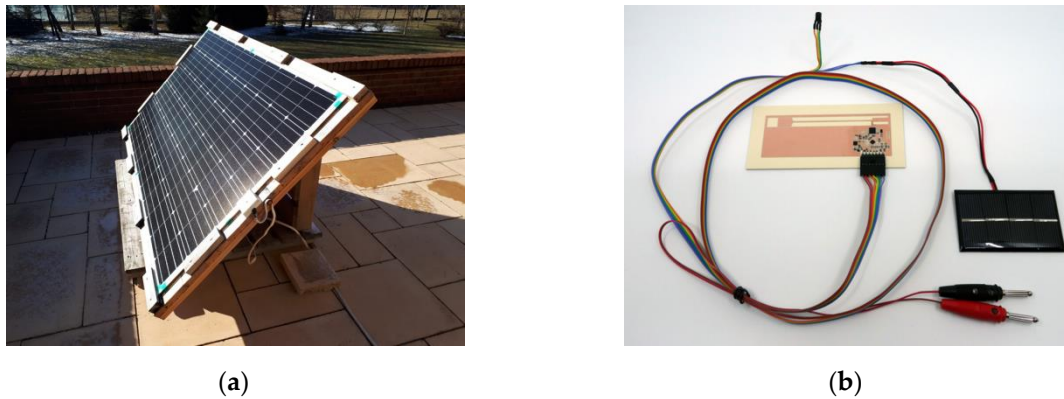


Figure 12. Outside tests: (a) measurement application; (b) test sample of RFID sensor with external sensors.

In order to implement the scenarios discussed, it is important to determine whether it is possible to obtain enough energy that is needed for a stable operation of the RFID sensor in the transition periods of the daily cycle: night/day and day/night. The algorithm for acquiring and, if necessary, processing of measurement data starts after crossing the selected threshold voltage V_{ON} . The daily cycle starts at this time and its length may vary from e.g., about 8 h to over 16 h (for the latitude of the experiment site). The end of the measurement procedure can be caused both by the end of the daily cycle (voltage drop below the V_{min} value) and the implemented scheme of the parameter sampling. From this perspective, the fragment of the $I_{PV} = f(V_{PV})$ characteristic (Figure 13a), which corresponds to a small current flow (approx. 5% of the rated current), is particularly interesting. In this interval, the PV module should be treated as unloaded due to the nature of the inverter operation; on the other hand, any disturbances in this area may result in an incorrect recognition of the new daily cycle.

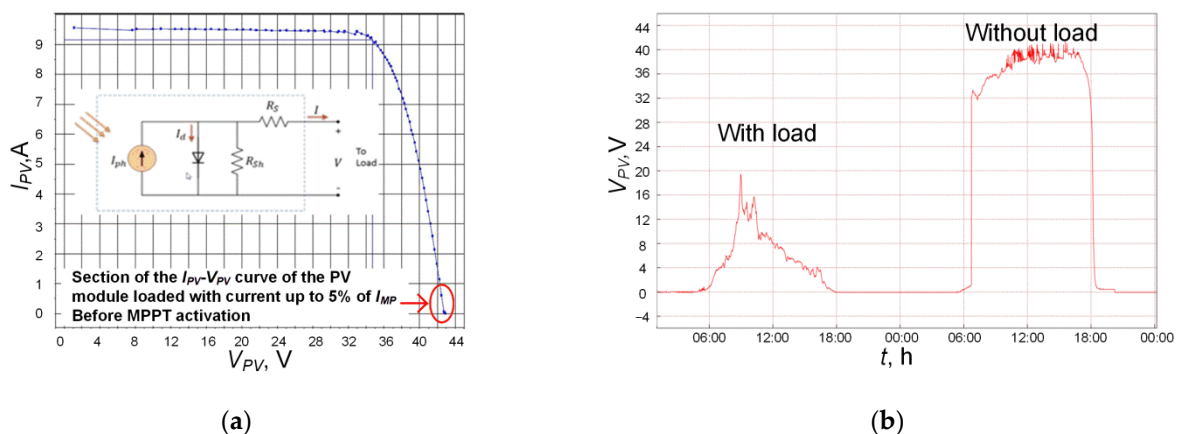


Figure 13. Characteristics of PV micro-power plant: (a) I_{PV} vs. V_{PV} of PV module; (b) V_{PV} vs. t of PV module with and without load at a similar level of low illumination (covered by snow in both scenarios).

The vast majority of inverters available commercially use the MPPT technique. This function ensures that the load impedance of the inverter is matched to the internal impedance of the PV module. The impedance dynamically changes with environmental conditions (mainly varying irradiance and temperature). Regardless of the MPPT algorithm used, the inverter continuously influences the output voltage of the PV module (Figure 13b). It starts working at the $V_{MPPTmin}$ value, which is equal to 13 V for the Skymax Expert MEX 1.5K-12 (this is the lowest $V_{MPPTmin}$ value in commercial devices). This value limits the upper

range of V_{ON} , which is the acceptable voltage level for safe activation of the measurement block. The lower voltage V_{min} limit is equal to 5 V, which is the minimum value at which the power unit in the RFID sensor can provide enough energy to the electronic circuits. Nevertheless, the activity of the MEAS Part can be easily extended beyond the daily cycle using a capacitive energy storage element—this prevents the influence of sudden weather phenomena causing temporary strong shading of the PV modules.

The $V = f(t)$ waveform at the output of the PV module is shown in Figure 14a. The PV module operates under changing loads generated by the inverter. In the absence of solar radiation, the voltage is below $V_{MPPTmin}$, and then no energy is received by the system. After reaching $V_{MPPTmin}$, the inverter attempts to load the PV module (Figure 14b). The attempts are made regularly with the minimum possible load until the voltage no longer drops below the MPPT threshold. With a further increase in irradiation, the system gradually increases the load to maintain the possible highest current under given conditions (Figure 14c). Although the inverter tries to maximize the power drawn from the PV module, the optimization of the maximal power point is still not achieved. Only a sufficient intensity of sunlight causes activation of the MPPT algorithm (Figure 14d). Note that the output voltage never drops below the MPPT threshold value (13 V in the experimental case) in the daily cycle, unless there is a complete absence of lighting, which is a very rare case.

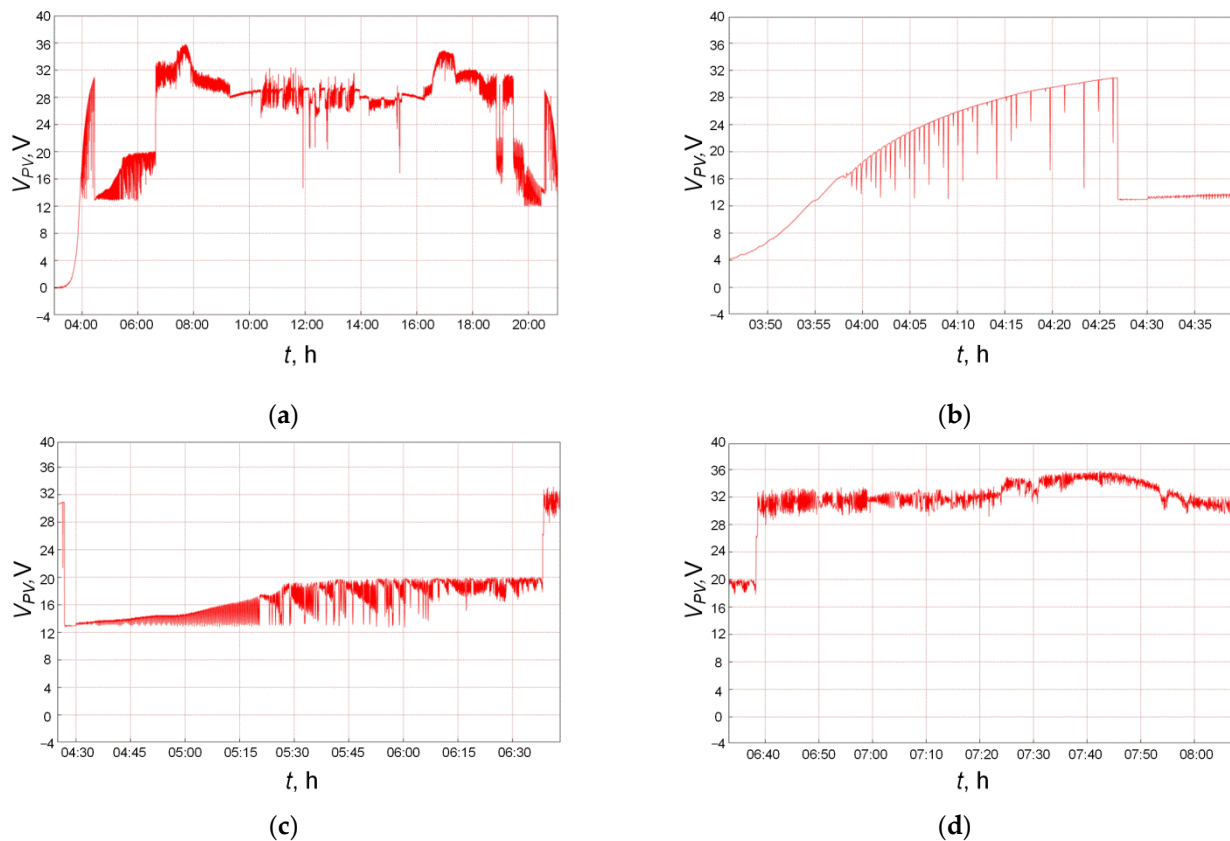


Figure 14. V_{PV} vs. t of the PV module loaded by Skymax inverter: (a) daily characteristic; (b) beginning period of daily characteristic at low solar irradiance and low load; (c) start of inverter under nominal load; (d) nominal operation of inverter with active MPPT function.

By stretching the waveform from Figure 14d, the operation of the MPPT algorithm can be observed (Figure 15a). The inverter is constantly trying to change the load to obtain the maximum power from the PV module. The sensor sampling is too sparse to accurately show the operation of the inverter algorithm. However, this does not prevent the diagnostics of damaged modules. The measurements taken by 10 test RFID sensors at the same time are shown in Figure 15b. They all follow the output voltage very closely,

reflecting the nature of the inverter's operation. The difference in the indications does not exceed 0.1 V.

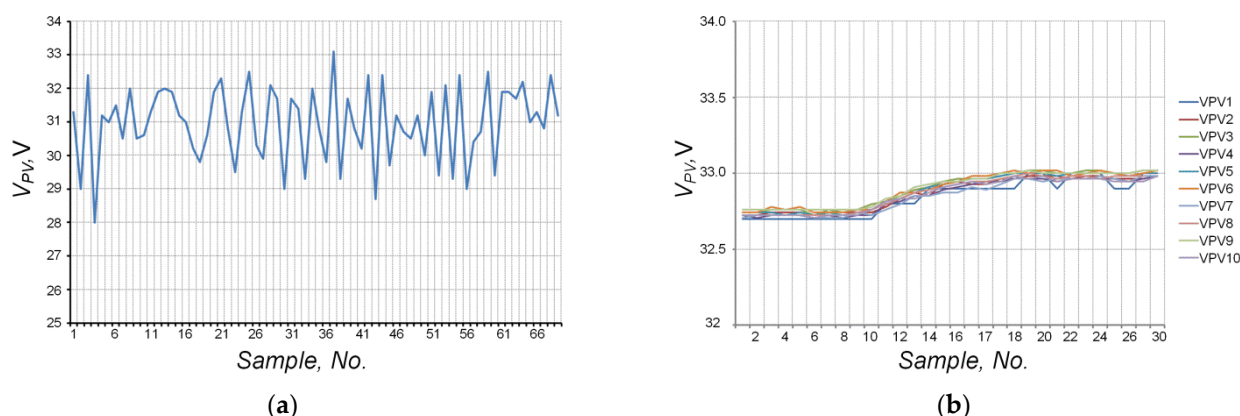


Figure 15. V_{PV} vs. sample No. of PV module loaded by Skymax inverter: (a) nominal operation of inverter with active MPPT function in short period of time; (b) voltage at PV module terminals measured by test RFID sensors.

4. Conclusions

All proposed concepts of the supervision system are based on the RFID technology. Although, for the considered measuring devices, the illuminated PV module with a power of several hundred watts is an inexhaustible source of energy, and the use of active radio devices for data transmission would not be a problem in such power conditions, the use of the RFID sensor has some advantages. The RFID transponder can be read even if the PV cells are broken or completely darkened. The acquired data can be available to the service technicians even after the facade element is disassembled, and when the photovoltaic installation is completely damaged.

It should be noted that the proposed demonstrator can be used to obtain a universal device that may be applied to any package, regardless of the type of PV cells used. It is also consistent with the solutions commonly used in the RFID technology.

The proposed RFID sensor is designed to work with the marked object during its entire life cycle: in the stages of production, distribution (in supply chains), installation (at the end user), operation, service/maintenance, disposal, etc. This means that, throughout this cycle, there will be no need to use other RFID transponders that are additionally attached to the object. Moreover, access to the information saved in the internal memory of the tag can be provided wirelessly at every stage of the life cycle.

Although all the integrated electronic circuits of the RFID sensor demonstrator can be replaced with other components with similar functional properties, some design steps have to be undertaken again in order to obtain an efficient device. In this context, the RFID chip is the most important element. The SL900A was selected to carry out the tests in question. Depending on the advancement of the measurement part and the work scenario, the RFID sensor structure will be more or less complicated. In the simplest case, it is possible to use only the built-in additional blocks of the RFID chip. In the most complex solution, it is necessary to use a microcontroller (or PLD) to supervise the measurement processes, data processing and transmission, energy management, etc. In addition, it should be noted that the analytical software supplemented with an appropriate database containing detailed information about the configuration and structure of the monitored facility can be used for a significant simplification of the RFID sensor circuitry.

Supplementary Materials: The following supporting information can be downloaded at: <https://www.mdpi.com/article/10.3390/en15041401/s1>. Scheme S1: Integrated analog monitor rev.3.

Author Contributions: Conceptualization, M.W. and C.C.; methodology, P.J.-M. and M.W.; software, G.P. and P.P.; validation, K.K. and C.C.; formal analysis, G.P. and W.L.; investigation, P.P. and M.C.; resources, W.L. and G.P.; data curation, M.C. and P.P.; writing—original draft, M.W. and K.K.; writing—review and editing, M.W. and P.J.-M.; visualization, P.P. and M.C.; supervision, P.J.-M. and K.K.; project administration, M.W.; funding acquisition, P.J.-M. All authors have read and agreed to the published version of the manuscript.

Funding: This research paper was developed under the project financed by the Minister of Education and Science of the Republic of Poland within the “Regional Initiative of Excellence” program for years 2019–2022. Project number 027/RID/2018/19, amount granted 11 999 900 PLN.

Institutional Review Board Statement: Not applicable.

Informed Consent Statement: Not applicable.

Data Availability Statement: All calculated and measured data will be provided upon request to the correspondent authors by email with appropriate justification.

Conflicts of Interest: The authors declare no conflict of interest. The funders had no role in the design of the study; in the collection, analyses, or interpretation of data; in the writing of the manuscript, or in the decision to publish the results.

References

1. Pilkington. Glass Handbook 2014. Available online: <https://www.pilkington.com> (accessed on 22 August 2021).
2. Węglarski, M.; Jankowski-Miśkiewicz, P.; Chamera, M.; Dziejczak, J.; Kwaśnicki, P. Designing Antennas for RFID Sensors in Monitoring Parameters of Photovoltaic Panels. *Micromachines* **2020**, *11*, 420. [CrossRef] [PubMed]
3. Jankowski-Miśkiewicz, P.; Węglarski, M.; Lichoń, W.; Chamera, M.; Pyt, P.; Ciejka, C. Synthesis of Antennas for Active Glazing Unit with Photovoltaic Modules. *Energies* **2021**, *14*, 6632. [CrossRef]
4. van Sark, W. PV System Design and Performance. *Energies* **2019**, *12*, 1826. [CrossRef]
5. Reinders, A.; Verlinden, P.; van Sark, W.; Freundlich, A. *Photovoltaic Solar Energy: From Fundamentals to Applications*, 1st ed.; John Wiley & Sons, Ltd.: Chichester, UK, 2017; p. 720.
6. Tian, H.; Mancilla-David, F.; Ellis, K.; Muljadi, E.; Jenkins, P. *Detailed Performance Model for Photovoltaic Systems: Preprint*; Report No NREL/JA-5500-54601/TRN: US201217%256; National Renewable Energy Lab. (NREL): Golden, CO, USA, 2012; pp. 30–41.
7. Mariano, J.R.L.; Lin, Y.-C.; Liao, M.; Ay, H. Analysis of Power Generation for Solar Photovoltaic Module with Various Internal Cell Spacing. *Sustainability* **2021**, *13*, 6364. [CrossRef]
8. Kim, J.; Rabelo, M.; Padi, S.P.; Yousuf, H.; Cho, E.-C.; Yi, J. A Review of the Degradation of Photovoltaic Modules for Life Expectancy. *Energies* **2021**, *14*, 4278. [CrossRef]
9. Fan, Y.; Fang, L.; Wu, H.; Liu, B.; Huang, J.; Lin, S.; Wang, Z.; Wang, Y. A Novel Cascaded Modular Photovoltaic Energy Storage System for Partial Shading Conditions. *Appl. Sci.* **2021**, *11*, 5552. [CrossRef]
10. Paredes-Parra, J.M.; Mateo-Aroca, A.; Silvente-Niñirola, G.; Bueso, M.C.; Molina-García, Á. PV Module Monitoring System Based on Low-Cost Solutions: Wireless Raspberry Application and Assessment. *Energies* **2018**, *11*, 3051. [CrossRef]
11. Ansari, S.; Ayob, A.; Lipu, M.S.H.; Saad, M.H.M.; Hussain, A. A Review of Monitoring Technologies for Solar PV Systems Using Data Processing Modules and Transmission Protocols: Progress, Challenges and Prospects. *Sustainability* **2021**, *13*, 8120. [CrossRef]
12. Mallor, F.; León, T.; De Boeck, L.; Van Gulck, S.; Meulders, M.; Van der Meerssche, B. A method for detecting malfunctions in PV solar panels based on electricity production monitoring. *Solar Energy* **2017**, *153*, 51–63. [CrossRef]
13. Finkenzeller, K. *RFID Handbook—Fundamentals and Applications in Contactless Smart Cards, Radio Frequency Identification and Near-Field Communication*, 3rd ed.; Wiley: Hoboken, NJ, USA, 2010.
14. Han, P.; Zhang, Z.; Xia, Y.; Mei, N. A 920 MHz Dual-Mode Receiver with Energy Harvesting for UHF RFID Tag and IoT. *Electronics* **2020**, *9*, 1042. [CrossRef]
15. Unander, T.; Nilsson, H. Evaluation of RFID based sensor platform for packaging surveillance applications. In Proceedings of the IEEE International Conference on RFID-Technologies and Applications, Sitges, Spain, 15–16 September 2011; pp. 27–31. [CrossRef]
16. Deriche, M.; Raad, M.W.; Suliman, W. An IOT based sensing system for remote monitoring of PV panels. In Proceedings of the 16th International Multi-Conference on Systems, Signals Devices (SSD), Istanbul, Turkey, 21–24 March 2019; pp. 393–397. [CrossRef]
17. Slapšak, J.; Mitterhofer, S.; Topič, M.; Jankovec, M. Wireless System for In Situ Monitoring of Moisture Ingress in PV Modules. *IEEE J. Photovolt.* **2019**, *9*, 1316–1323. [CrossRef]
18. Jankowski-Miśkiewicz, P.; Węglarski, M. Definition, Characteristics and Determining Parameters of Antennas in Terms of Synthesizing the Interrogation Zone in RFID Systems. In *Radio Frequency Identification*, 1st ed.; Crepaldi, P.C., Pimenta, T.C., Eds.; INTECH: London, UK, 2017; Chapter 5; pp. 65–119. [CrossRef]

19. GS1 EPCglobal. *EPC Radio-Frequency Identity Protocols Generation-2 UHF RFID*; Specification for RFID Air Interface Protocol for Communications at 860 MHz–960 MHz, ver. 2.1; EPCglobal: Brussels, Belgium, 2018.
20. European Telecommunications Standards Institute. *ETSI EN 302 208*; Radio Frequency Identification Equipment Operating in the Band 865 MHz to 868 MHz with Power Levels up to 2 W and in the Band 915 MHz to 921 MHz with Power Levels up to 4 W; European Telecommunications Standards Institute: Valbonne, France, 2016.
21. Code of Federal Regulations. Title 47. Telecommunication. Part 15.247 Operation within the bands 902–928 MHz, 2400–2483.5 MHz, and 5725–5850 MHz. Published by the Office of the Federal Register National Archives and Records Administration as a Special Edition of the Federal Register, October 2020. Available online: <https://www.govinfo.gov/app/details/CFR-2010-title47-vol1/CFR-2010-title47-vol1-sec15-247> (accessed on 10 January 2022).
22. Węglarski, M.; Jankowski-Mihułowicz, P. Factors Affecting the Synthesis of Autonomous Sensors with RFID Interface. *Sensors* **2019**, *19*, 4392. [[CrossRef](#)] [[PubMed](#)]
23. AMS. *SL900A EPC Class 3 Sensory Tag Chip—For Automatic Data Logging*; Datasheet; AMS: Premstaetten, AG, Austria, 2018; Available online: <http://ams.com> (accessed on 10 February 2020).
24. Suresh, K.; Jeoti, V.; Soeung, S.; Drieberg, M.; Goh, M.; Aslam, M.Z. A Comparative Survey on Silicon Based and Surface Acoustic Wave (SAW)-Based RFID Tags: Potentials, Challenges, and Future Directions. *IEEE Access* **2020**, *8*, 91624–91647. [[CrossRef](#)]
25. Torres-Torres, D.; Torres-Torres, C.; Vega-Becerra, O.; Cheang-Wong, J.C.; Rodríguez-Fernández, L.; Crespo-Sosa, A.; Oliver, A. Structured strengthening by two-wave optical ablation in silica with gold nanoparticles. *Opt. Laser Technol.* **2015**, *75*, 115–122. [[CrossRef](#)]
26. Farsens: ROCKY100—EPC C1G2 Compliant UHF RFID Tag with Power Harvesting and SPI Communication for External Low Power Sensors and Actuators, Datasheet, DS-ROCKY100-V01, September 2017. Available online: <http://www.farsens.com/wp-content/uploads/2017/12/DS-ROCKY100-V04.pdf> (accessed on 10 January 2022).
27. EM Microelectronic-Marin SA: EM4325—18000-63 Type C (Gen2) and 18000-63 Type C/18000-64 Type D (Gen2/TOTAL) RFID IC, 4325-DS, Ver. 9.0, September 2017. Available online: https://www.emmicroelectronic.com/sites/default/files/products/datasheets/4325-ds_0.pdf (accessed on 10 January 2022).
28. Cypress: *WM72016-6 16Kbit Secure F-RAM Memory with Gen-2 RFID Access & Serial Port Direct Memory Access*. Document Number: 001-86227; Cypress Semiconductor Corp. 2013. Available online: <https://www.cypress.com/file/120726/download> (accessed on 10 January 2022).
29. Jankowski-Mihułowicz, P.; Węglarski, M. Determination of Passive and Semi-Passive Chip Parameters Required for Synthesis of Interrogation Zone in UHF RFID Systems. *Elektron. Elektrotech.* **2014**, *20*, 65–73. [[CrossRef](#)]